AFOSR - TR - 77 - 0256

AD A038078

FINAL TECHNICAL REPORT

to the

AIR FORCE OFFICE OF SCIENTIFIC RESEARCH

from

Eugene Herrin

and

Tom Goforth

Dallas Geophysical Laboratory
Southern Methodist University
Dallas, Texas 75275

Approved for public release;
distribution unlimited.

ARPA Order: 2382
Program Code: 4F10
Name of Contractor: Southern Methodist University
Effective Date of Contract: February 1, 1973
Contract Expiration Date: July 15, 1976
Total Amount of Contract Dollars: $711,731
Contract Number: F44620-73-C-0044, P00005
Principal Investigator and Phone Number: Eugene Herrin
AC 214 692-2760
Program Manager and Phone Number: Truman Cook, Director of
Research Administration
AC 214 692-2031

Title of Work: The Detection and Research of Rayleigh and Love Waves

University Account Number: 80-58

DDC FILE COPY

Sponsored by
Advanced Research Projects Agency
ARPA Order No. 2382

DDC
RECEIVED
APR 8 1977
D

AIR FORCE OFFICE OF SCIENTIFIC RESEARCH (AFSC)
NOTICE OF TRANSMITTAL TO DDC
This technical report has been reviewed and is approved for public release IAW AFR 190-12 (7b).
Distribution is unlimited.
A. D. BLOSE
Technical Information Officer

UNCLASSIFIED

SECURITY CLASSIFICATION OF THIS PAGE (When Data Entered)

REPORT DOCUMENTATION PAGE	READ INSTRUCTIONS BEFORE COMPLETING FORM
1. REPORT NUMBER: AFOSR - TR - 77 - 0256	2. GOVT ACCESSION NO. / 3. RECIPIENT'S CATALOG NUMBER
4. TITLE (and Subtitle): THE DETECTION AND RESEARCH OF RAYLEIGH AND LOVE WAVES.	5. TYPE OF REPORT & PERIOD COVERED: Final Rept.
	6. PERFORMING ORG. REPORT NUMBER
7. AUTHOR(s): Eugene Herrin, Tom Goforth	8. CONTRACT OR GRANT NUMBER(s): F44620-73-C-0044, new ARPA Order - 2382
9. PERFORMING ORGANIZATION NAME AND ADDRESS: Dallas Geophysical Laboratory, Southern Methodist University, Dallas TX 75275	10. PROGRAM ELEMENT, PROJECT, TASK AREA & WORK UNIT NUMBERS: 62701E 4F10, 2382-06
11. CONTROLLING OFFICE NAME AND ADDRESS: ARPA, 1400 Wilson Blvd., Arlington VA22209	12. REPORT DATE: Feb 1977
	13. NUMBER OF PAGES: 35 (37 p.)
14. MONITORING AGENCY NAME & ADDRESS (if different from Controlling Office): AFOSR/NP, Bolling AFB, Bldg.#410, Wash DC 20332	15. SECURITY CLASS. (of this report): Unclassified
	15a. DECLASSIFICATION/DOWNGRADING SCHEDULE

16. DISTRIBUTION STATEMENT (of this Report)

Approved for public release; distribution unlimited.

17. DISTRIBUTION STATEMENT (of the abstract entered in Block 20, if different from Report)

407 712

18. SUPPLEMENTARY NOTES

TECH OTHER

19. KEY WORDS (Continue on reverse side if necessary and identify by block number)

20. ABSTRACT (Continue on reverse side if necessary and identify by block number)

Phase-matched filters are defined as a class of linear filters in which the Fourier phase of the filter is made equal to that of a given signal. An interative technique is described which can be used to find a phase-matched filter for a particular seismic signal. The process is then applied to digital records of Rayleigh waves from a synthetic source with propagation across 55 deg. of continental path, an earthquake in the Greenland Sea recorded in Texas, and a nuclear explosion in Novaya Zemlya recorded in New Mexico. → next page

DD FORM 1 JAN 73 1473 EDITION OF 1 NOV 65 IS OBSOLETE

UNCLASSIFIED

SECURITY CLASSIFICATION OF THIS PAGE (When Data Entered)

Application of the filter allows multiple arrivals to be identified and removed and allows recovery of the complex spectrum of the primary wave train along with its apparent group velocity dispersion curve. The amplitude spectrum of the primary signal obtained by this linear spectrum of the primary signal obtained by this linear process is not contaminated by interference from multipath arrivals. The filtering process also provides significant improvement in signal-to-noise ratio; greater than factor of four for the Greenland Sean and Novaya Zemlya events.

White Section ☑
Buff Section ☐
☐
DISTRIBUTION/AVAILABILITY CODES
Dist. AVAIL. and/or SPECIAL
A

PHASE-MATCHED FILTERS: Application to the Study of Rayleigh Waves

DDC
RECEIVED
APR 8 1977
D

Eugene Herrin and Tom Goforth
Geophysical Laboratory
Southern Methodist University
February 1977

DISTRIBUTION STATEMENT A
Approved for public release;
Distribution Unlimited

ABSTRACT

Phase-matched filters are defined as a class of linear filters in which the Fourier phase of the filter is made equal to that of a given signal. An iterative technique is described which can be used to find a phase-matched filter for a particular seismic signal. The process is then applied to digital records of Rayleigh waves from a synthetic source with propagation across 55 deg. of continental path, an earthquake in the Greenland Sea recorded in Texas, and a nuclear explosion in Novaya Zemlya recorded in New Mexico. Application of the filter allows multiple arrivals to be identified and removed and allows recovery of the complex spectrum of the primary wave train along with its apparent group velocity dispersion curve. The amplitude spectrum of the primary signal obtained by this linear process is not contaminated by interference from multipath arrivals. The filtering process also provides significant improvement in signal-to-noise ratio; greater than a factor of four for the Greenland Sea and Novaya Zemlya events.

ACKNOWLEDGEMENTS

The writers wish to thank George McKinley, Eugene Smart, Billie Kimball, Craig Woerpel and Nancy Cunningham who have worked extensively on the computer code used in the phase-matching process. Funds for this research were provided by the Advance Research Project Agency under contract AFOSR F44620-73-C-0044 monitored by the U.S. Air Force Office of Scientific Research.

INTRODUCTION

Matched Filters

The matched filter has been defined by Turin (1960, p. 311) as follows: Given any physical waveform, s(t), then the filter matched to s(t) is, by definition, one with the impulse response

$$h(\tau) = ks(\Delta - \tau), \tag{1}$$

where k and Δ are arbitrary constants. In equation (1), when we consider τ to have the units of time, then Δ denotes a shift in time. We can consider the factor k to be 1 and apply a shift in the time axis so that $\Delta = 0$. Thus the impulse response of the filter matched to s(t) is simply $s(-\tau)$. Convolution of the matched filter with the signal is

$$h(\tau) * s(t) = s(-\tau) * s(t) \Rightarrow |S(\omega)|^2 \exp i \left[-\sigma(\omega) + \sigma(\omega)\right] \tag{2}$$

where the symbol $\Rightarrow$ means ". . . has the Fourier transform . . ." Thus the right hand side is just $|S(\omega)|^2$. Now consider the cross-correlation of s(t) with its matched filter having the direction of time reversed

$$s(t) \otimes s(t) \Rightarrow |S(\omega)|^2 \exp i \left[\sigma(\omega) - \sigma(\omega)\right]$$

which is recognized as the auto-correlation of s(t). We see that the output obtained by filtering s(t) with $s(-\tau)$ is the same as that obtained by auto-correlating the signal, s(t).

Turin (1960, p. 312) shows that, in the presence of "white noise", the matched filtering process maximizes the signal to noise power ratio. In the following discussion we will assume that the instrument used to record seismic data, the seismograph, has an amplitude response that is approximately the inverse of the background noise, and thus the requirement for "white noise" is essentially met.

Phase-Matched Filters

We consider convolution and cross-correlation of a signal, $s(t)$, with a time function, $f(t)$, to be represented by the following operations and their Fourier transforms,

$$s(t) * f(\tau) \Rightarrow |S(\omega)| \, |F(\omega)| \quad \exp i\left[\sigma(\omega) + \phi(\omega)\right]$$

and

$$s(t) \otimes f(t) \Rightarrow |S(\omega)| \, |F(\omega)| \quad \exp i\left[\sigma(\omega) - \phi(\omega)\right]. \quad (3)$$

Now suppose that we choose $f_p(t)$ such that the Fourier phase is the same as that of $s(t)$. We define the class of linear operators, $f_p(t)$, such that $\sigma(\omega) = \phi_p(\omega)$, as phase-matched filters with respect to the signal, $s(t)$. The output of the second of the above operations will then have the Fourier transform, $|S(\omega)| \, |F_p(\omega)|$, and will be an even function in the time domain as is the auto-correlation function. The output of the first operation, convolution, with the direction of time reversed, that is, $f_p(-\tau)$ substituted for $f_p(t)$, will

have the same Fourier transform. We call this output, whether obtained by filtering or correlation, a pseudo-autocorrelation function (PAF). If means can be found for matching the Fourier phase of the signal and the filter, then the time domain output, the PAF, will depend, for a given signal, only upon the amplitude spectrum of the particular phase-matched filter used in the operation.

Now consider some possible choices for $|F_p(\omega)|$.

$$|F_p(\omega)| = |S(\omega)| \qquad \text{(a)}$$

$$|F_p(\omega)| = 1 \qquad \text{(b)}$$

$$|F_p(\omega)| = \frac{1}{|S(\omega)|} \qquad \text{(c)}$$

If choice (a) is made, the phase-matched filter becomes the matched filter and maximizes the signal to noise power ratio assuming "white noise". If we were using a power detector to indicate the presence of a low-level signal, choice (a) should give the best results. In this case the PAF becomes the autocorrelation function. On the other hand, choice (c) is simply the inverse filter and the PAF becomes the impulse function. In practice, choice (c) would maximize the time resolution of the output, but would greatly reduce the signal to noise ratio (Turin, 1960, p. 318). If our problem is one of low signal to noise ratio we should use a filter spectrum approximating choice (a), but if we have interfering signals, all with large signal to noise ratios, a spectrum approaching

that in choice (c) would be more appropriate. In the following examples we have used choice (b), a convenient compromise between maximum signal to noise improvement and maximum time resolution.

The above relationships result from the use of infinite integrals and continuous functions in the time and frequency domains. The results, however, hold for practical applications involving finite sums and sampled functions provided proper precautions are taken to avoid wrap-around and aliasing in computing finite Fourier transforms.

APPLICATIONS TO RAYLEIGH WAVES

Alexander and Lambert (1971) discuss the application of matched filters to the analysis of surface waves and to the determination of their amplitude spectra. They show that by "pre-whitening" the matched filter the length of the output function was reduced by about a factor of two. They state (p. 7) that "the only negative feature of the whitened matched filter is that as a detector it will be less satisfactory than the unwhitened filter." In fact, they were using a phase-matched filter, as defined in the previous section, with an amplitude spectrum, $|F(\omega)|$, approximately equal to 1 over the band of interest. The length of the PAF was halved thus the time resolution was twice that of the matched-filter.

Alexander and Lambert (1971) did not show how to obtain the matched filter when the exact form of the signal is unknown. In this section we describe an iterative technique which can be used to find a phase-matched filter for a given seismic signal. The process is then applied to digital records of Rayleigh waves.

Table 1 is a flow diagram of the computer code we use in the phase-matching process. We assume that the seismic signals result from a dispersive process with a continuous dispersion

TABLE 1
FLOW DIAGRAM

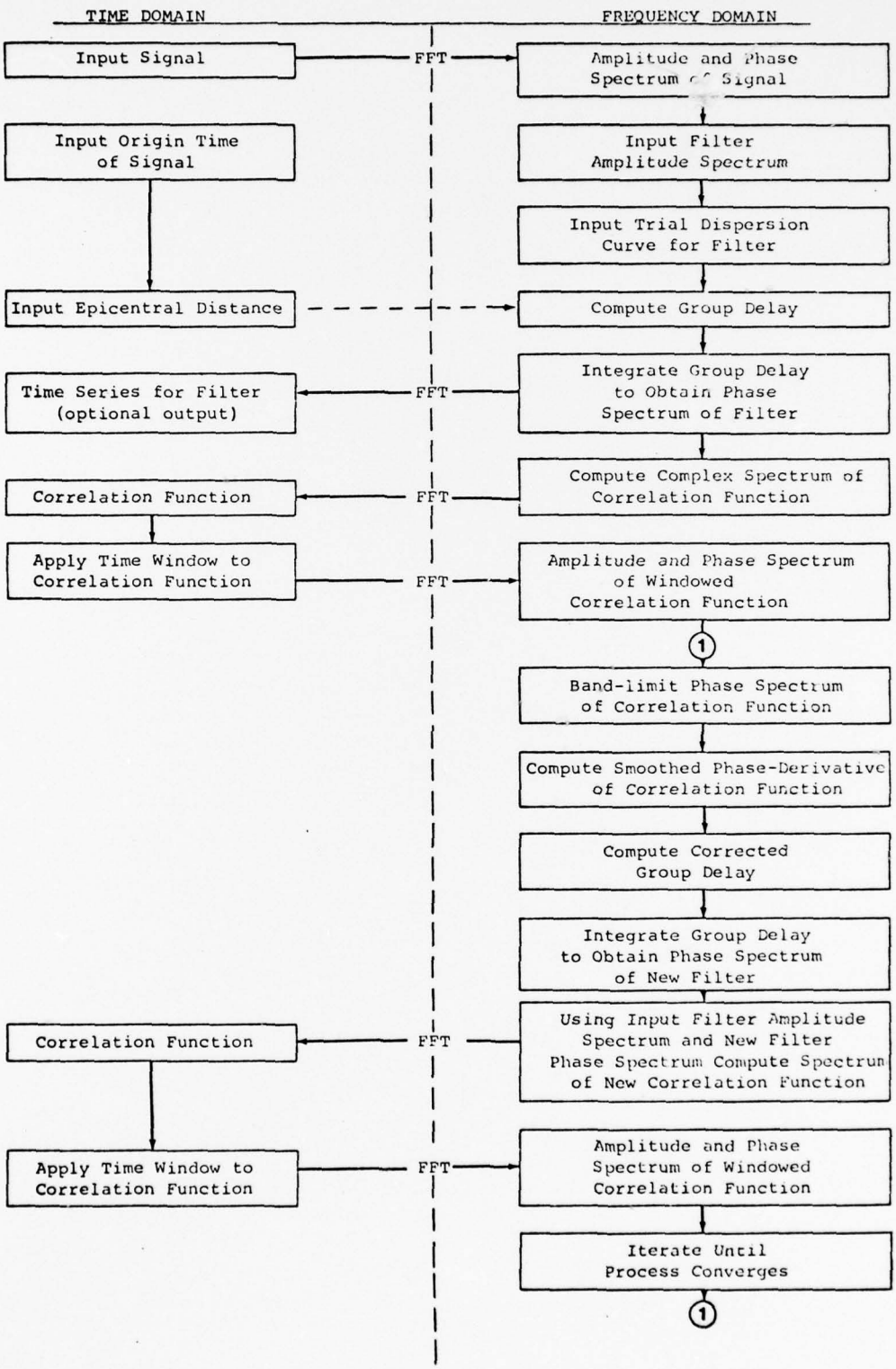

curve (group velocity vs. frequency). The group delay, $t_{gr}(\omega)$, associated with the signal is the epicentral distance divided by the group velocity at frequency ω. From Papoulis (1962, p. 134) we note that the group delay and Fourier phase of the signal are related as follows:

$$t_{gr}(\omega) = \frac{d\,\Theta(\omega)}{d\,\omega} \tag{4a}$$

and

$$\Theta(\omega_1) = \int_0^{\omega_1} t_{gr}(\omega)\, d\,\omega\,. \tag{4b}$$

In the code the signal is Fourier transformed to obtain the amplitude and phase spectra. These finite transforms involve only positive times and frequencies so that, in practice, time shifts of $\frac{T}{2}$ and phase shifts of exp $\left[-i\,\frac{T}{2}\,\omega\right]$, where T is the length of the time domain window, must be taken into account. We provide as input a trial group velocity dispersion curve and an amplitude spectrum for the filter. Using the epicentral distance to the signal source and Eq. (4b) we compute the Fourier phase of f(t) and perform the correlation in the frequency domain (Eq. 3). The result is then transformed to the time domain, windowed to reject correlation functions from interfering signals or multipath arrivals, then transformed again. The result will have the complex spectrum

$$|S(\omega)|\;|F(\omega)|\quad \exp i\left[\sigma(\omega) - \phi(\omega)\right]. \tag{5}$$

We then "unwind" the difference in Fourier phases, $\sigma(\omega)-\phi(\omega)$,

which in practice is multiplied by the linear phase shift associated with the offset in the lag domain window, and obtain a smoothed estimate of its derivative. The smoothing process assumes that the first derivative of the dispersion curve is continuous; hence, by Eq. 4a, the second derivative of the Fourier phase spectrum must be continuous. This estimate is used to correct the group delay of the trial filter (Eq. 4a). The process is repeated until the phase spectra of the filter and the desired signal in the band of interest are identical. We have then obtained the phase-matched filter, $f_p(t)$, having the given amplitude spectrum, $|F_p(\omega)|$. The spectrum of the signal can be recovered because the Fourier transform of the resulting PAF is $|S(\omega)||F_p(\omega)|$. In the following examples the filter spectrum is "whitened"; that is, $|F_p(\omega)| = 1$ in the frequency band of interest (periods of 10 to 100 seconds).

Synthetic Signal

In order to demonstrate the application of the phase-matching process to dispersed surface waves, a synthetic signal with overlapping multipath arrivals was constructed. Fig. 1 shows schematically the plan in this construction. Path 1 is followed by the direct or primary arrival, whereas paths 2 and 3 represent reflections. The source-strength is assumed to vary azimuthally so that arrivals 1 and 2 have comparable

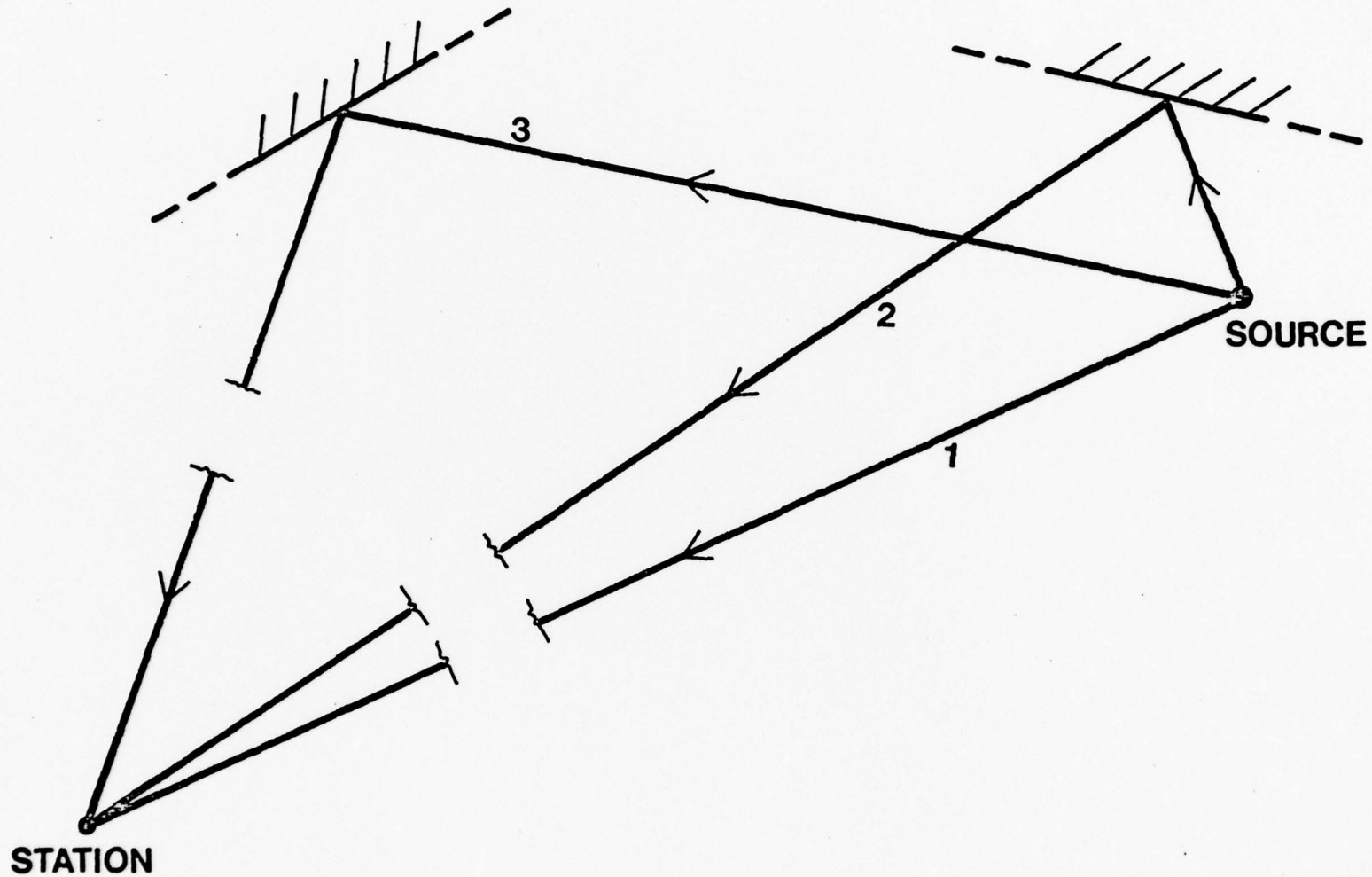

Fig. 1

Schematic diagram showing propagation paths for the synthetic signal.

strength. Arrival 3 has about ¼ the amplitude of the other two. The time separations are 100 sec between arrivals 1 and 2 and 300 sec between 1 and 3. The same dispersion curve was used to generate all three arrivals, but because of the difference in path-lengths the group delays and Fourier phases of the arrivals will be different. Fig. 2 shows the synthetic signal for an epicentral distance of 55 deg. The Airy phase for the second arrival can be seen but the end of the third arrival is not shown.

The trial dispersion curve used as input to the phase-matching code was significantly different from the one used to generate the synthetic signal. Fig. 3 shows the correlation functions generated in four iterations of the code. An iterative procedure is required because the smoothing process used in the estimation of the Fourier phase derivative is numerically damped and because the operator may change control parameters during the calculation. Pass 1 in Fig. 3 shows the correlation function obtained using the trial dispersion curve. Multipathing is definitely indicated so the operator chose a fairly narrow lag window centered on the predicted arrival time of Rayleigh energy with greater than 100 sec. period. The window was narrowed on subsequent passes, and in Pass 4 a nearly perfect PAF was obtained; that is, the phase of the primary signal was matched within the limitations of accuracy imposed by the sampling rate (1 per sec.). After

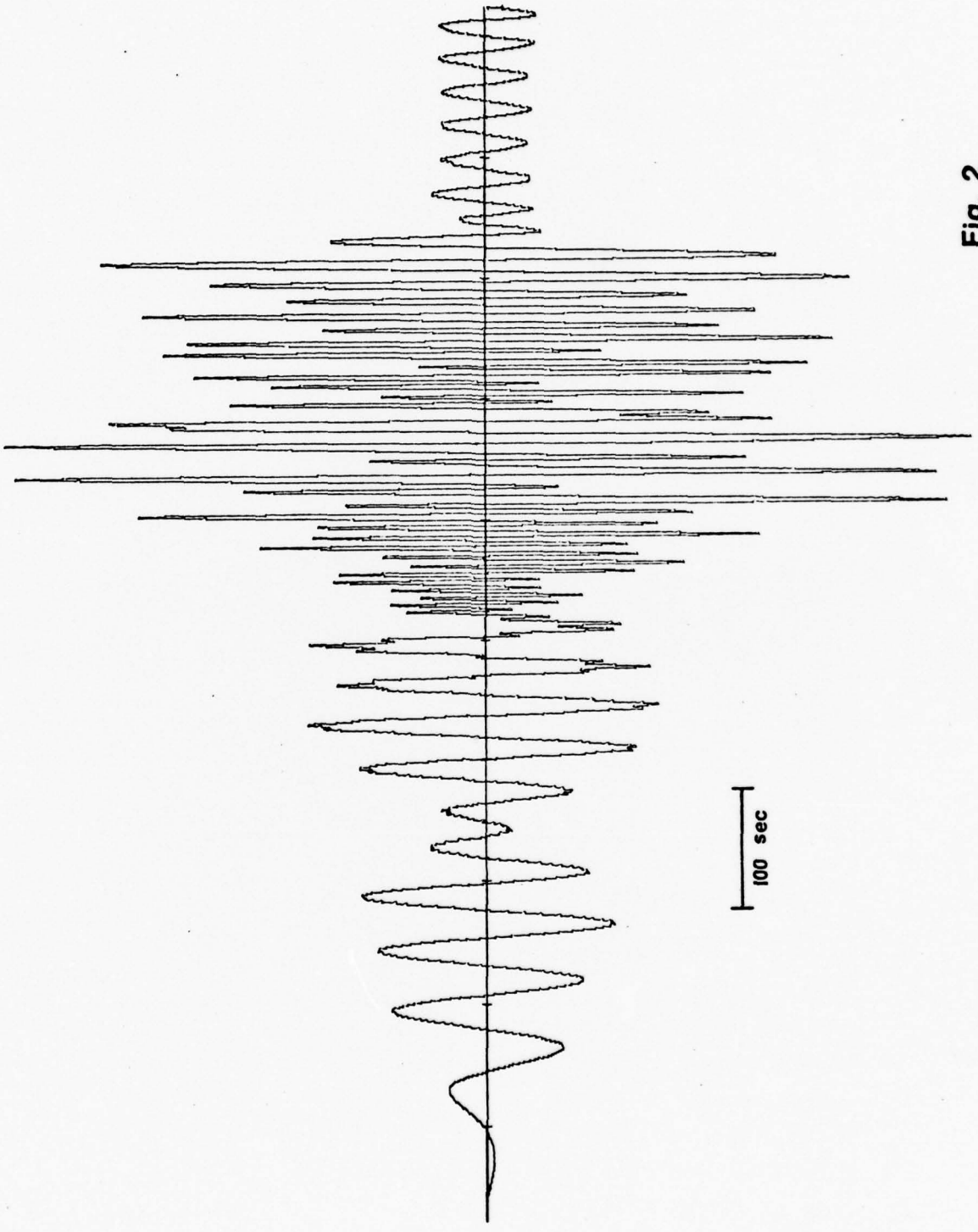

Fig. 2

The synthetic signal.

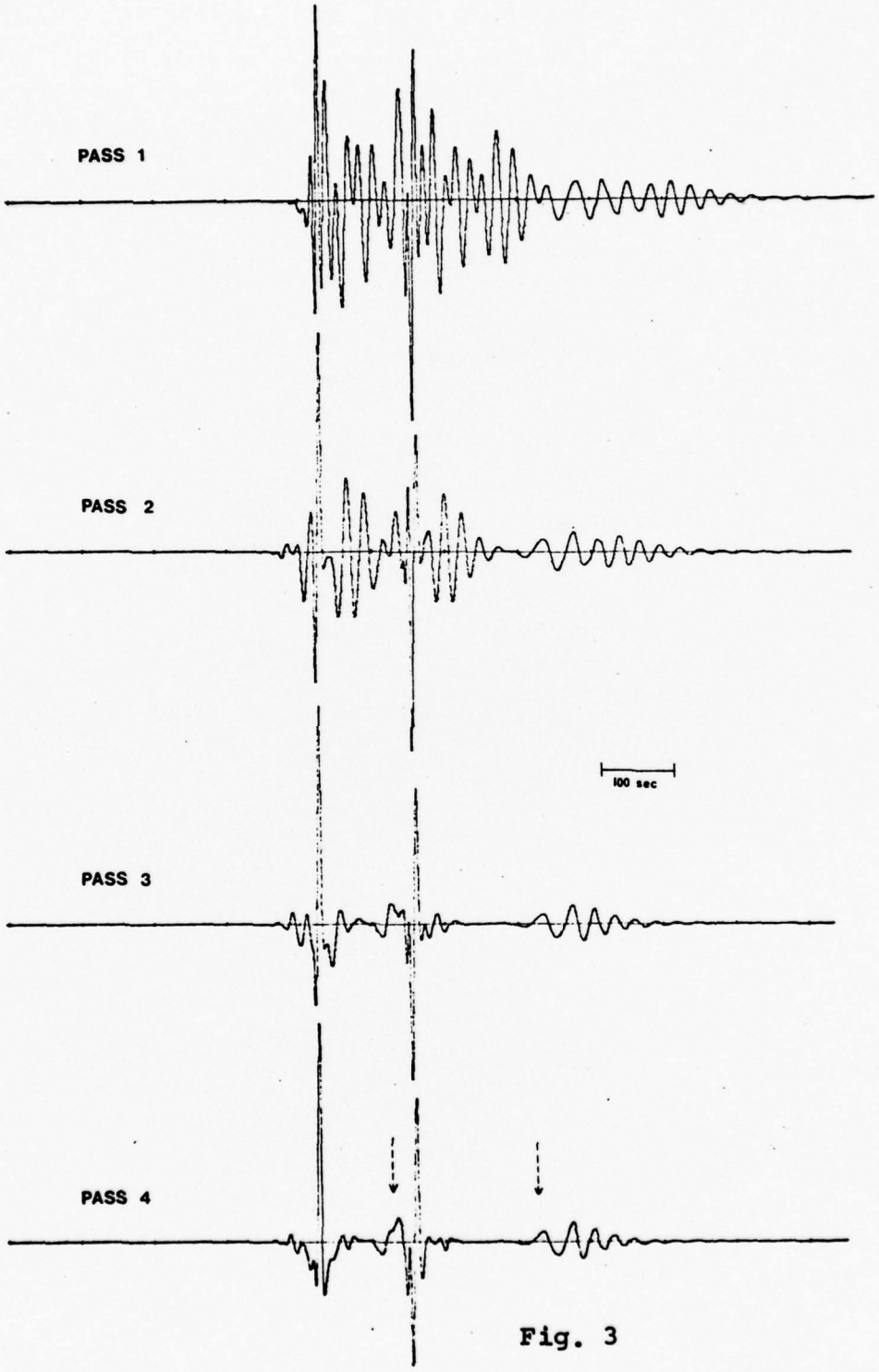

Fig. 3

The cross-correlation functions from four iterations of the phase-matching code operating on the synthetic signal. The dashed lines show the time of arrival of the second and third components of the signal.

the final iteration essentially all the primary energy has been compressed into about 50 sec. of lag time. The correlation functions for arrivals 2 and 3 show that the filter is not phase-matched to these arrivals because their group delays are different from that of the primary. In Fig. 3, Pass 4, note the correlation functions for the second and third arrivals are displaced to the right of the actual arrival times, as shown by the dashed lines, because of the longer travel paths. This effect helps in extracting the primary energy when the separation times between arrivals becomes less than about 50 sec. The amplitude spectrum of the primary was recovered by taking the Fourier transform of the windowed correlation function of Pass 4.

Fig. 4 shows the starting (solid line) and final (dashed line) dispersion curves for the primary arrival in the synthetic signal. The dashed curve agrees with the one used to construct the synthetic signal within ± 0.005 km/sec. This test demonstrates the use of the filtering process to resolve overlapping signals, but without the presence of noise. The next example uses data from an earthquake with a significant amount of background noise present.

Greenland Sea Event

This particular signal, recorded from a vertical seismometer,

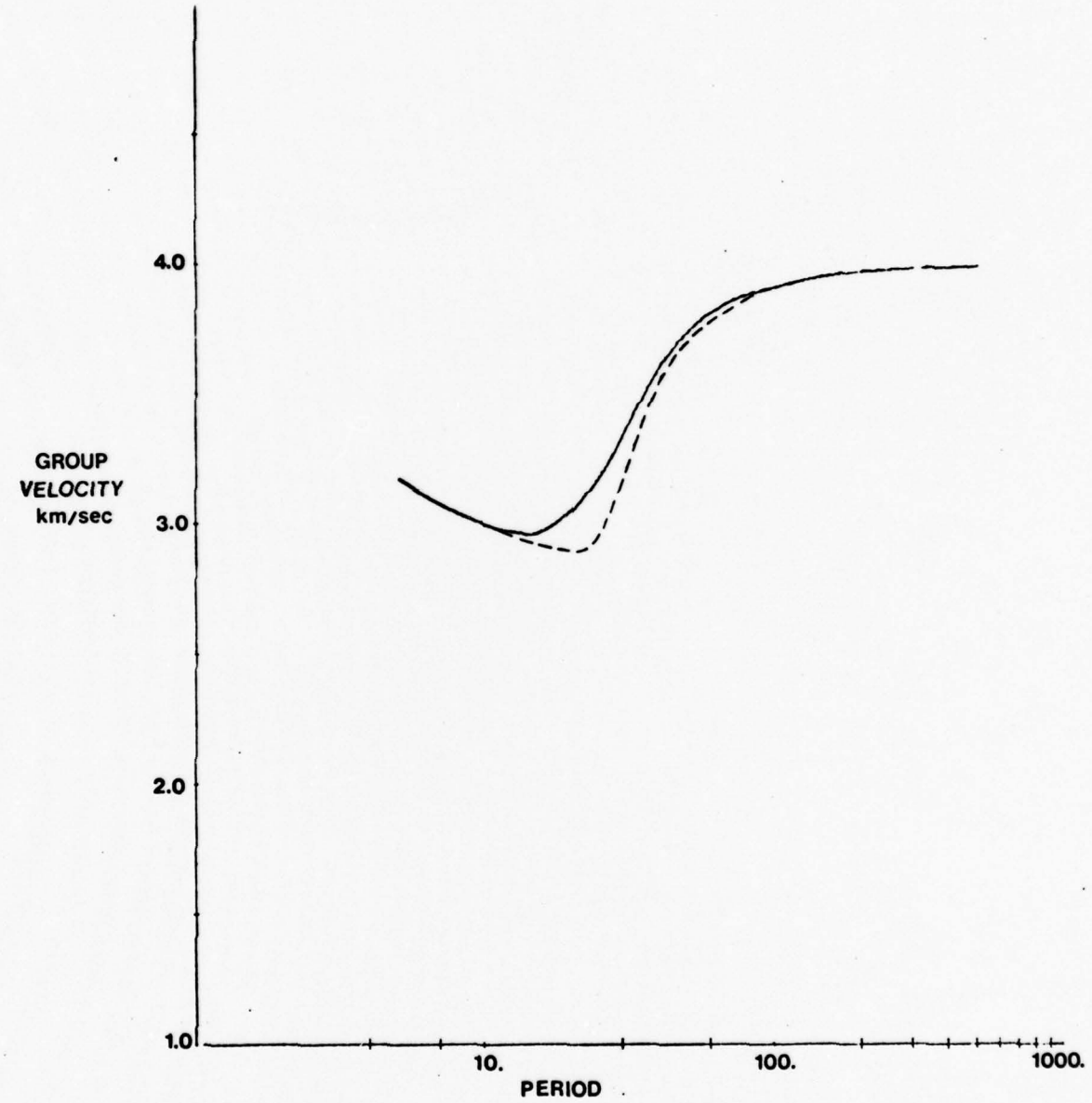

Fig. 4

The starting (solid line) and final (dashed line) dispersion curves for the synthetic signal.

was chosen because it shows very regular dispersion with almost no indication of multipath interference. Table 2 gives the pertinent data on this earthquake. The record was made in a salt mine at Grand Saline, Texas, using a long period seismometer with an amplitude response that is essentially the inverse of the background noise from periods of 10 to 100 sec. The spectra shown in this paper have not been corrected for instrument response.

A trial dispersion curve was selected and an initial filter was calculated in the frequency domain. This filter has an amplitude spectrum that is flat from periods of 4 sec. to 100 sec., thus the variations in amplitude seen in the time domain representation of the filter result from the properties of the dispersion curve (see Fig. 6).

Fig. 7 shows the correlation functions obtained in four iterations of the code. As the group delay, and hence the dispersion curve, was modified the correlation function approached a perfect PAF and an excellent phase-match was obtained. Fig. 8 shows the starting (solid line) and final (dashed line) dispersion curves for the Greenland Sea event. It must be emphasized that the final curve is an apparent, group velocity dispersion curve. We have not corrected the curve for the phase response of the instrument; furthermore, our studies on data from long period arrays (LASA and ALPA)

Table 2
Data pertinent to the earthquake
in the Greenland Sea

ORIGIN TIME	1970-139-02-07-41.5
LATITUDE	N 79.2 Deg.
LONGITUDE	E 2.5 Deg.
DEPTH	N
MAGNITUDE (m_b)	4.8
RECORDING SITE	Grand Saline, Texas
EPICENTRAL DISTANCE	59.70 Deg.

Table 3
Data pertinent to the nuclear explosion
in Novaya Zemlya, U.S.S.R.

ORIGIN TIME	1975-294-11-59-57.3
LATITUDE	N 73.35 Deg.
LONGITUDE	E 55.08 Deg.
DEPTH	0
MAGNITUDE (m_b)	6.5
RECORDING SITE	Albuquerque, New Mexico
EPICENTRAL DISTANCE	71.28 Deg.

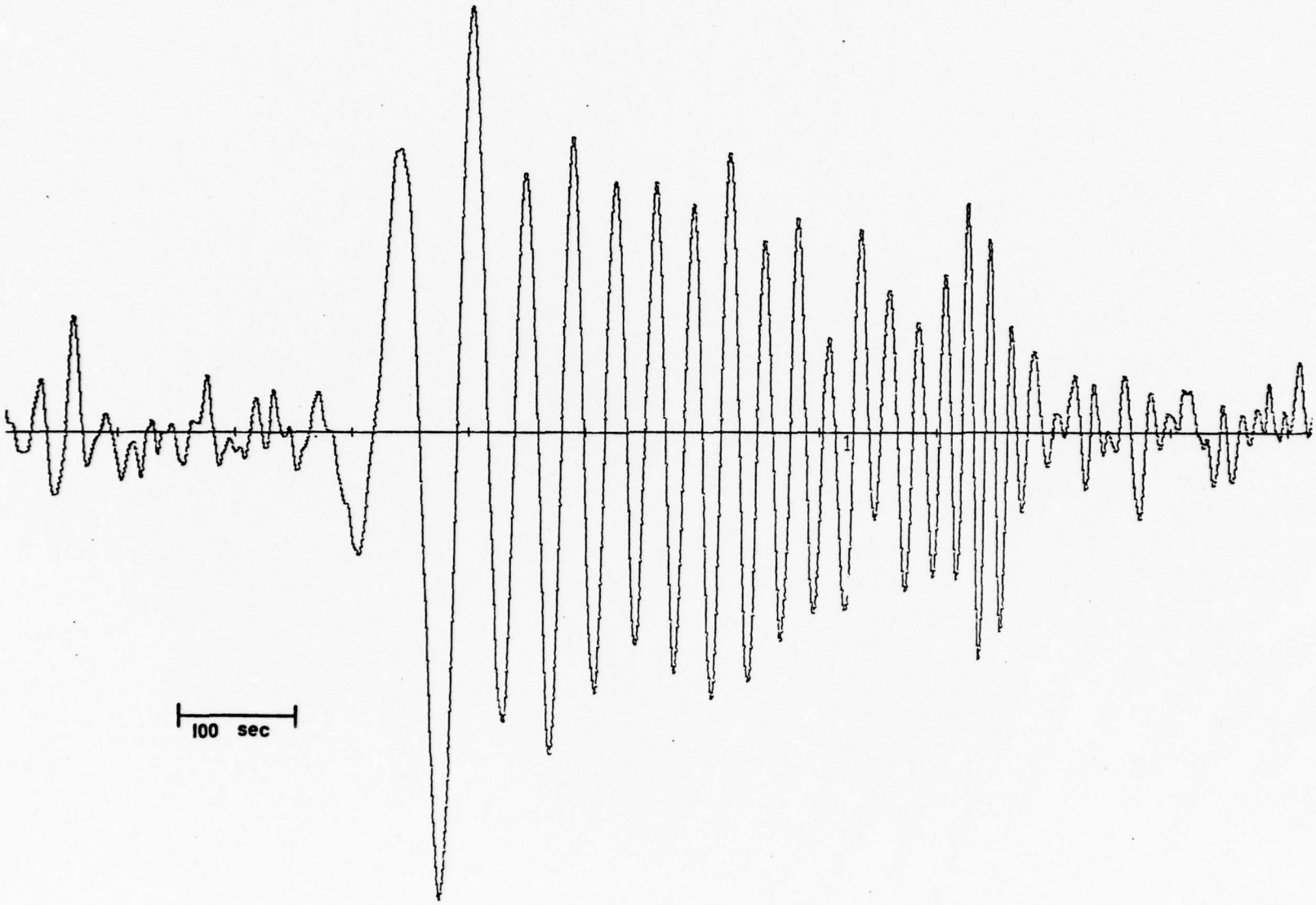

Fig. 5

The vertical component of the Rayleigh wave recorded from the Greenland Sea event (see Table 2).

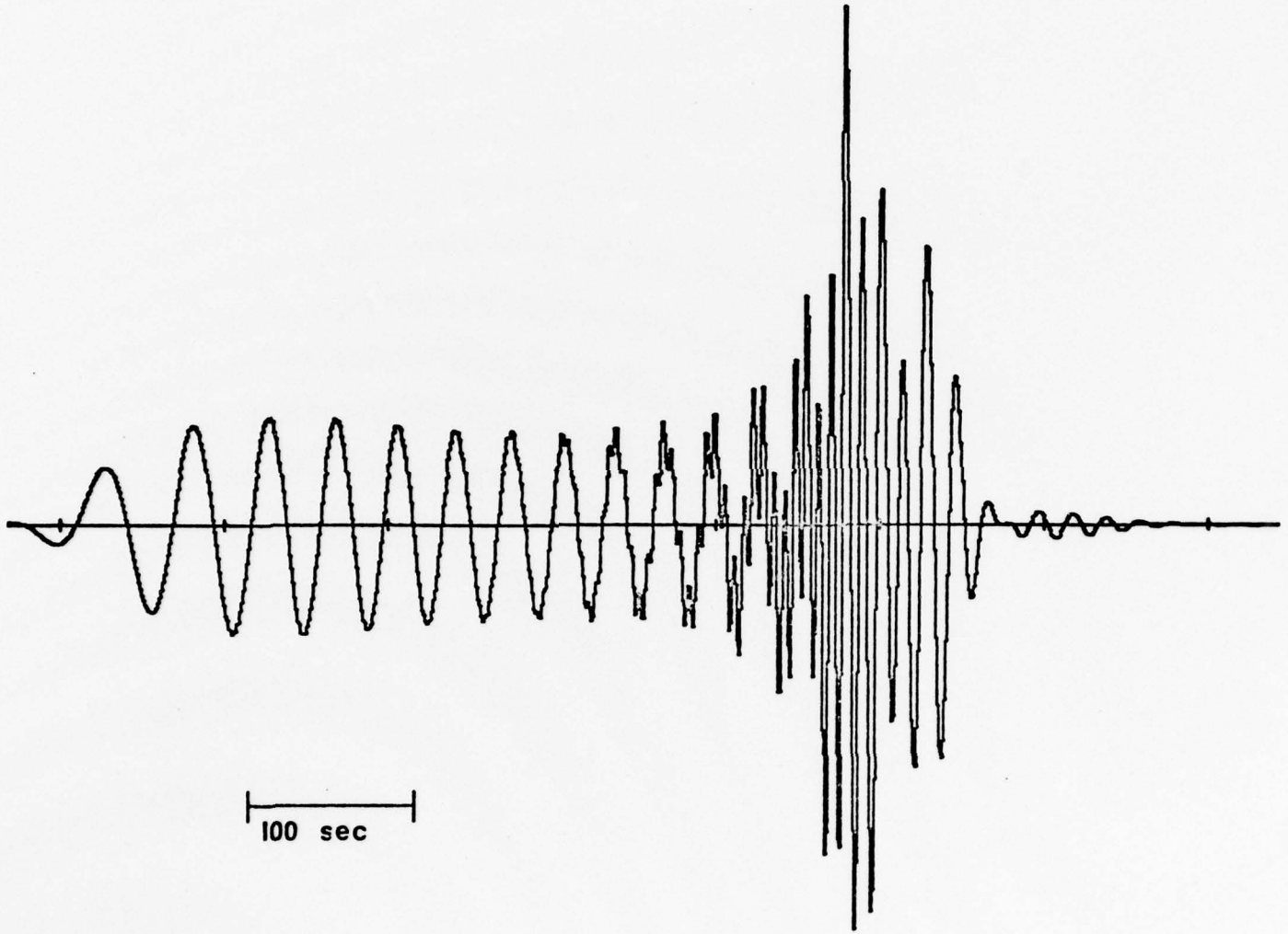

Fig. 6

One of the filters used in processing the Greenland Sea event.

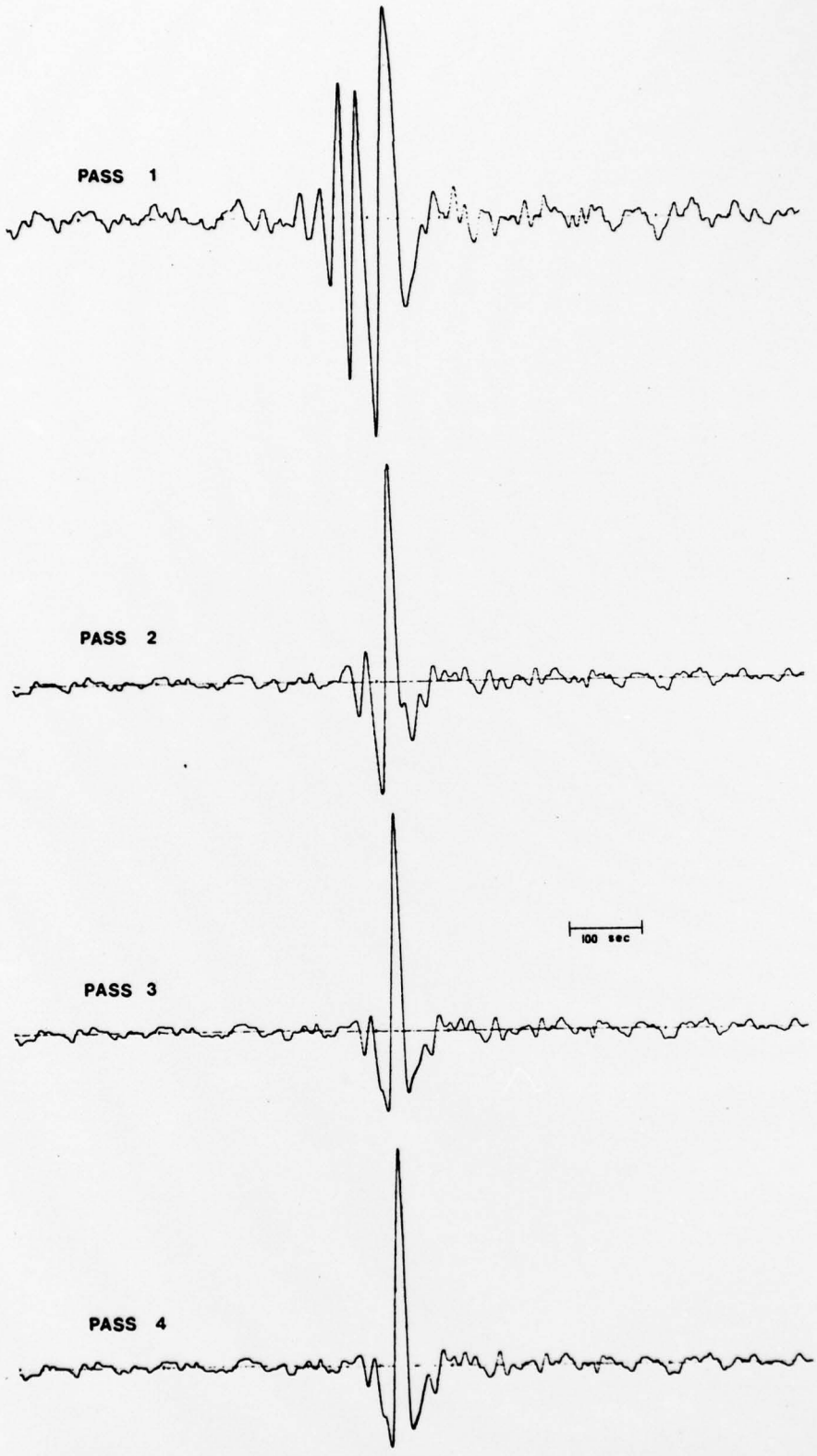

Fig. 7

The cross-correlation functions from four iterations of the phase-matching code operating on the Greenland Sea event.

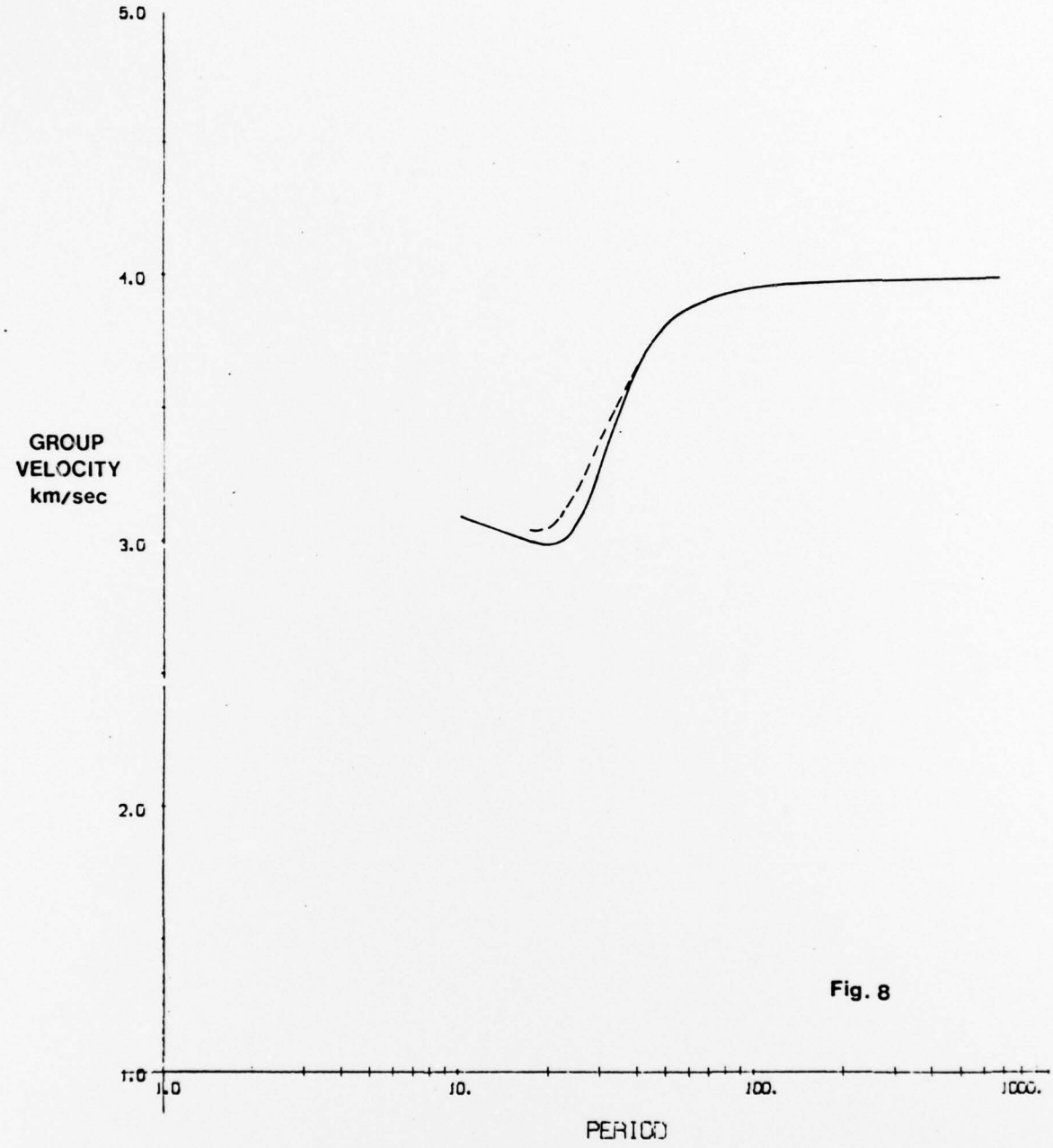

Fig. 8

The starting (solid line) and final (dashed line) dispersion curves for the Greenland Sea event.

show that even the primary arrival of Rayleigh energy may not follow a great circle path. These problems will be treated in detail in subsequent papers.

In Fig. 9 the amplitude spectrum of the windowed correlation function from Pass 4 (solid line) is superimposed on the spectrum (dashed line) obtained by transforming the entire signal shown in Fig. 5. There is some smoothing of the latter spectrum caused by the narrow lag window but the spectra are essentially the same. The spectral hole at a period of about 20 sec. is real; that is, the hole was not caused by multipath interference and is presumably indicative of the source spectrum. The filtering process has resulted in signal-to-noise improvement of greater than a factor of 4 in the band of interest (compare Figs. 5 and 7).

Novaya Zemlya Event

Fig. 10 shows the signal from the vertical module of a downhole, long period seismograph at Albuquerque, New Mexico (U.S.G.S.), for Rayleigh waves from an explosion in Novaya Zemlya, U.S.S.R. Pertinent data for this event are given in Table 3. The signal shows a beat pattern and an apparent repetition of the Airy phase which are indicative of multipath interference. A trial dispersion curve for the north polar path was chosen, and a whitened amplitude spectrum was then

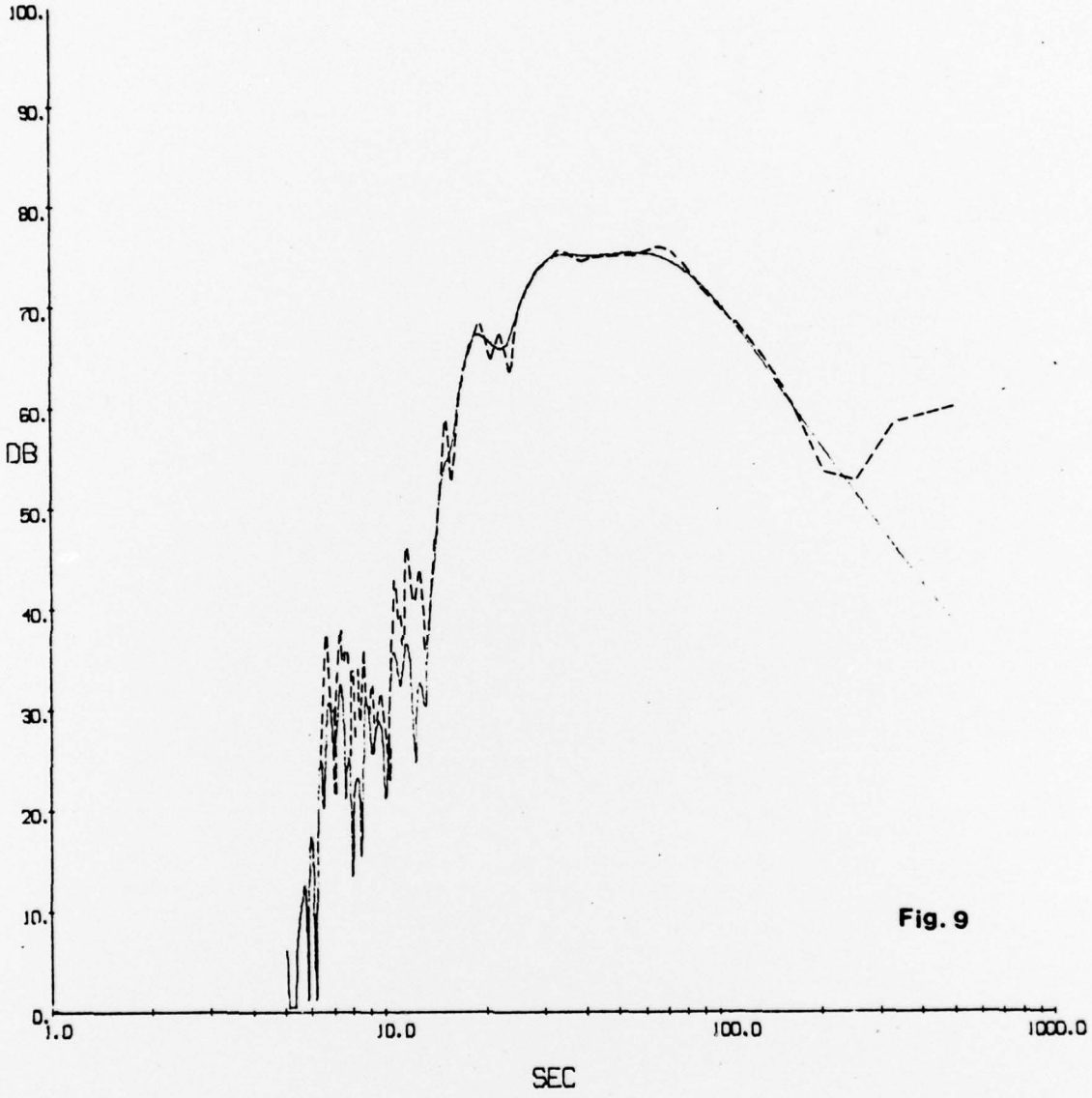

Fig. 9

The signal spectrum (dashed line) and the spectrum of the final correlation function (solid line) for the Greenland Sea event.

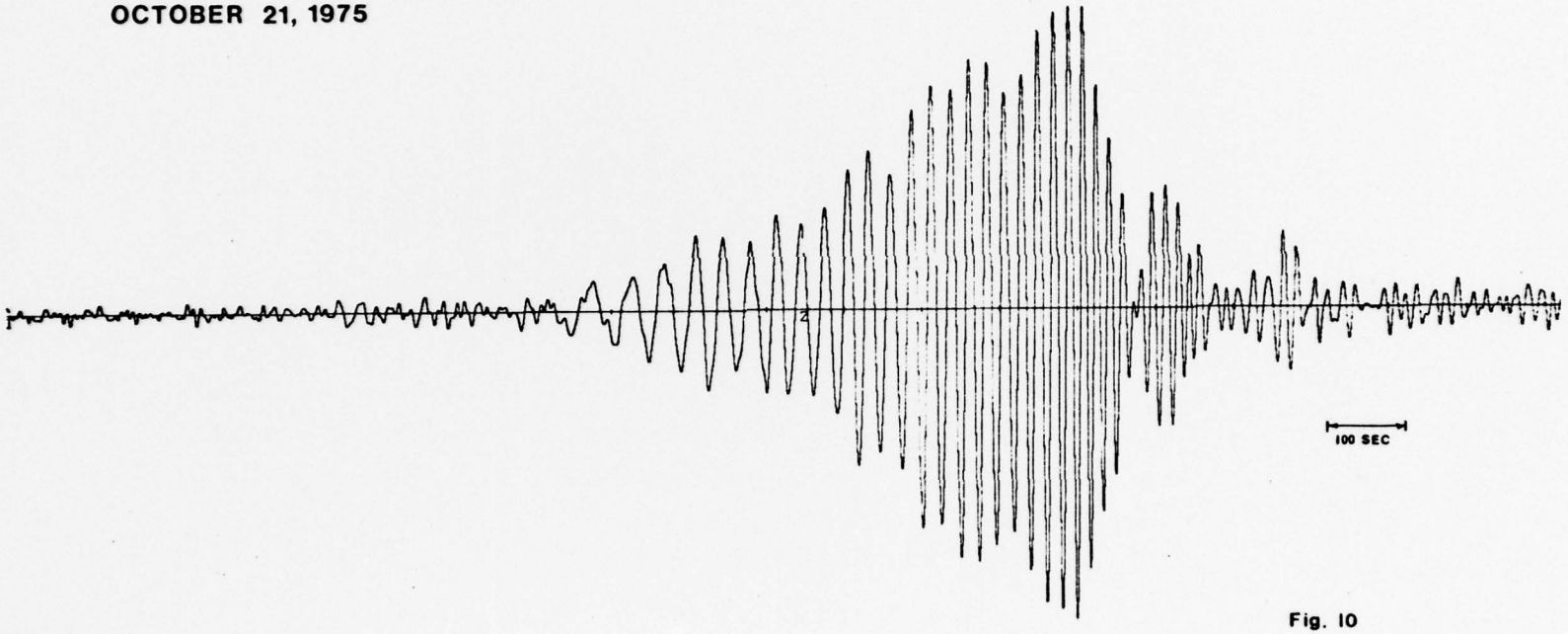

Fig. 10

The vertical component of the Rayleigh wave recorded from the Novaya Zemlya event (see Table 3).

used to construct the filter and perform the first correlation. The resulting correlation function and those for two subsequent passes are shown in Fig. 11. By Pass 3 an excellent PAF was obtained. The starting (solid line) and final (dashed line) dispersion curves are shown in Fig. 12.

There is a good indication of a second arrival 80 to 90 sec after the primary and another arrival about 170 sec later. Of course, the filter was not phase-matched to these later arrivals. The PAF from Pass 3 was windowed in the lag domain so as to exclude the second arrival but retain all of the primary correlation function. The signal spectrum (dashed line) and amplitude spectrum of the windowed PAF (solid line) are shown in Fig. 13. The ripple in the signal spectrum caused by multi-path interference has been removed by the filtering process.

Note that in Fig. 11, Pass 3, the total width of the PAF is only about 60 sec. so that a second arrival only 30 to 40 sec. after the primary could have been removed using the final filter. Even greater resolution may be obtained by modifying the amplitude spectrum of the filter so that the PAF approaches the band-limited impulse function as discussed in the first section of this paper.

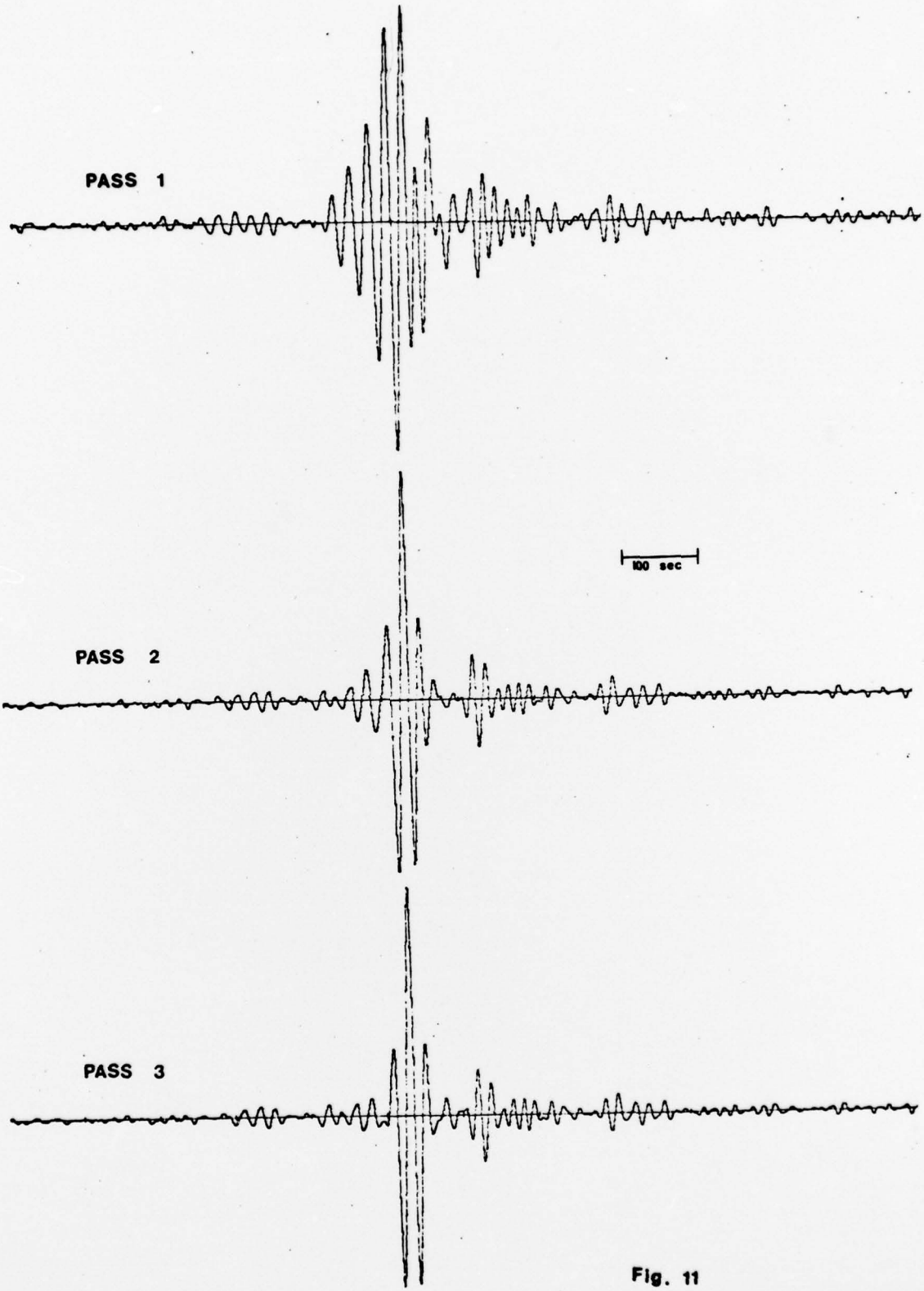

Fig. 11

The cross-correlation functions from three iterations of the phase-matching code operating on the Novaya Zemlya event.

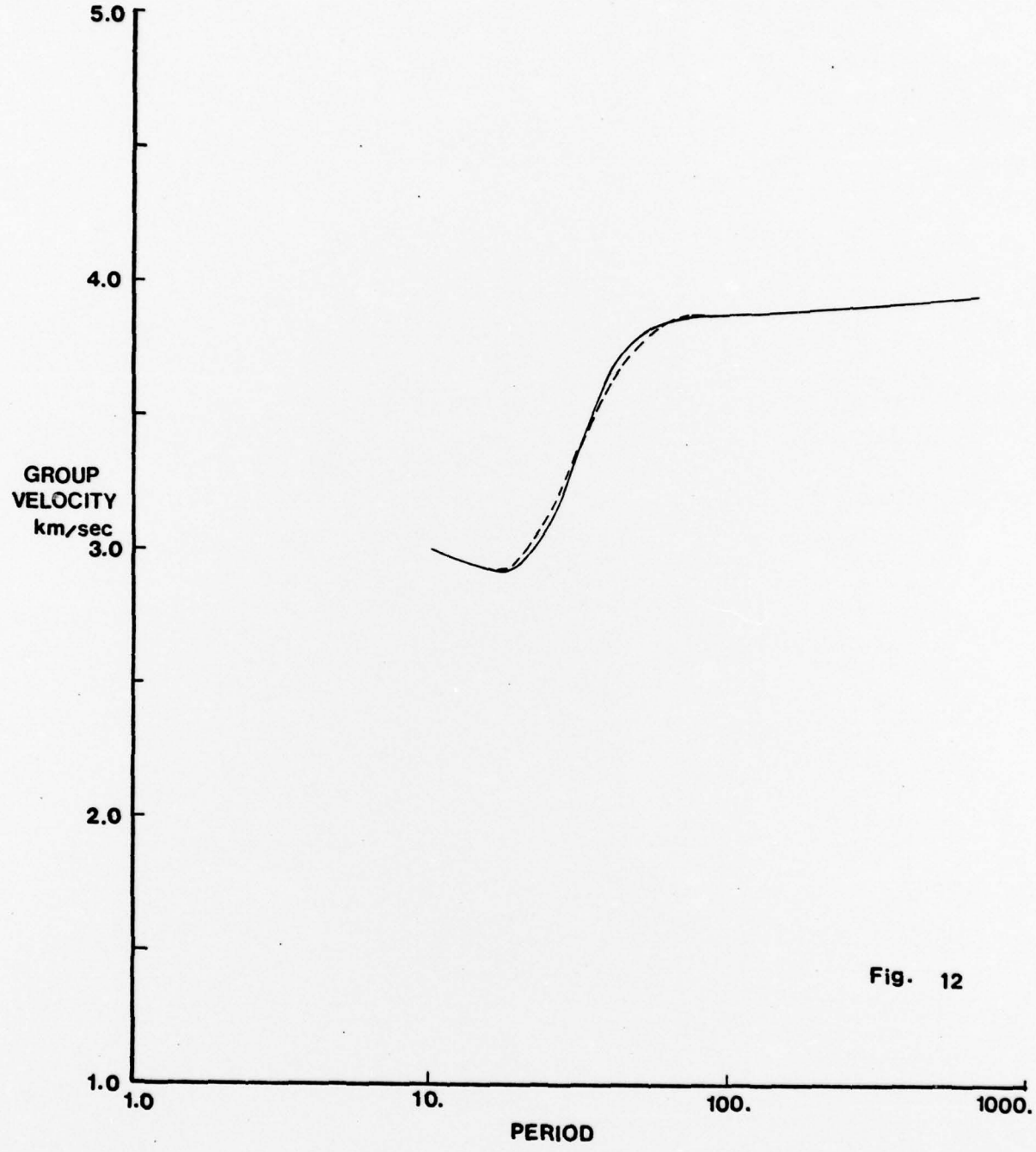

Fig. 12

The starting (solid line) and final (dashed line) dispersion curves for the Novaya Zemlya event.

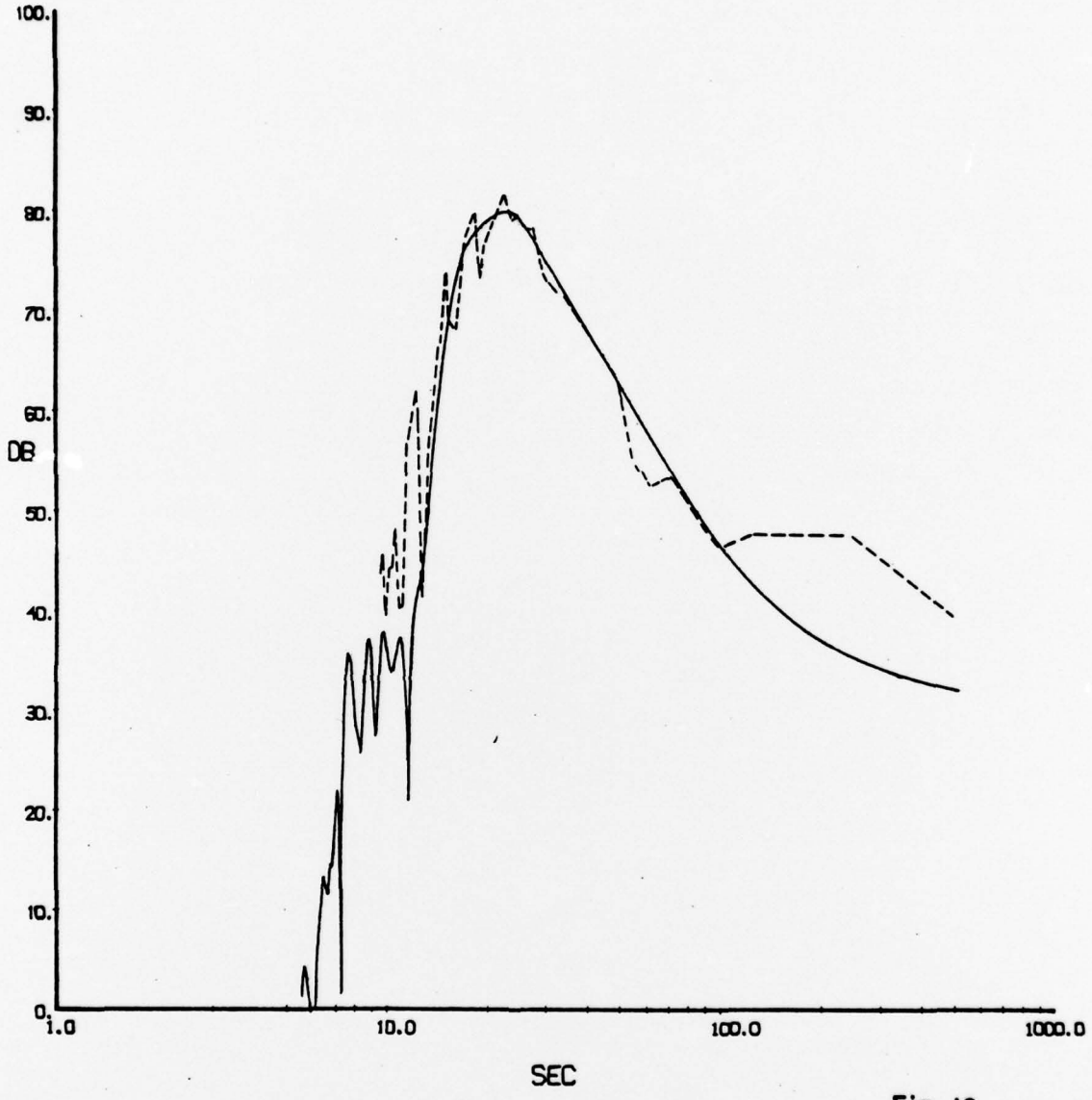

Fig. 13

The signal spectrum (dashed line) and spectrum of the final correlation function (solid line) for the Novaya Zemlya event.

DISCUSSION

The removal of the effects of multipaths using phase-matched filtering provides Rayleigh wave spectra which are much more closely related to source characteristics than are those obtained from Fourier transforms of the entire signal, and at the same time results in a substantial improvement in the signal to noise ratio. This process should provide the data necessary for studies relating surface wave spectra to focal parameters; give better estimates of surface wave magnitudes and their relationship to explosion yield; and permit re-evaluation of marginally successful techniques for explosion/earthquake discrimination such as depth determination from spectral nulls and the ratio of spectral amplitudes at periods of 20 and 40 seconds.

The whitened filter used on the Greenland Sea and Novaya Zemlya events is but one in a continuum of possible phase-matched filters. This filter appears to be a useful compromise between matched and inverse filters when the signal-to-noise ratio is moderate and the secondary arrivals lag the primary by at least 30 to 40 seconds. It has the obvious advantage of requiring no prior knowledge of the true amplitude spectrum of the signal.

The presence of multipaths in a surface wave train will bias conventional methods for determining apparent group velocity dispersion curves such that the estimates will be too slow. The removal of multipaths by phase-matched filtering removes this bias and thus improves the accuracy of the estimate. The precision of the phase-matched estimate is also improved in that known velocities of simulated signals can be recovered to within ± 0.005 km/sec.

The apparent dispersion curve obtained for the Greenland Sea event probably represents propagation along very nearly a great circle path. The source-station path for this event consists primarily of high-velocity shield and mid-continent regions, and it seems likely the great circle and least time paths coincide; however, there is no reason to believe that this is always true. Figure 14 shows the two paths and indicates that the Novaya Zemlya - Albuquerque great circle path traverses a part of the southern Rocky Mountains. When the great circle paths lie along or adjacent to major structural boundaries such as continental margins or mountain ranges, the possibility of the least-time path lying along another route must be considered. Such a circumstance may occur for many source-station pairs, and obviously complicates the problem of inverting apparent dispersion curves to obtain earth structure since the vertical velocity distribution would be confounded by lateral

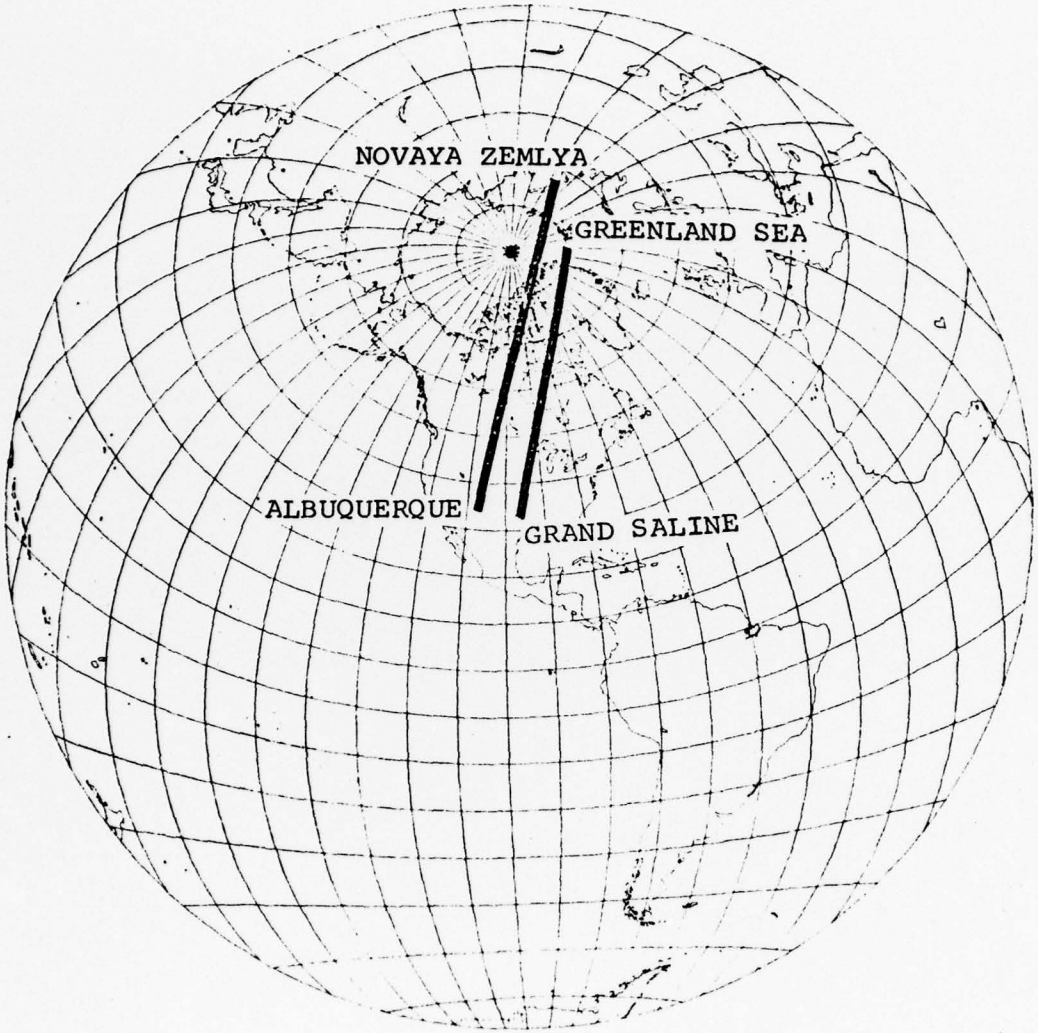

Fig. 14

A map showing the great circle paths for the Greenland Sea and Novaya Zemlya events.

inhomogenieties. Phase-matched filtering, with its ability to resolve overlapping dispersed wave trains into a series of impulse-like functions, offers a new approach to the surface wave inversion problem. A series of filtered seismograms representing various paths through a region can be interpreted in terms of positions of lateral boundaries in much the same way that deconvolved seismic reflection and refraction records can be used to locate velocity interfaces at depth. The complex spectra of the resolved multiple arrivals thus obtained can then be related to changes in physical properties at the interfaces.

Phase-matched filters have been applied to Rayleigh waves in this paper, but they would seem to have general applicability. Love wave signals are complicated by multipath Love arrivals as well as off-axis Rayleigh waves, hence phase-matched filtering should prove useful in their study. The application of these filters is not limited to signals which are strongly dispersed by the medium through which they travel, so that applications to the study of body waves are anticipated.

REFERENCES CITED

Alexander, S. S., and J. W. Lambert (1971) Single Station and Array Methods for Improved Surface Wave Spectral Estimates, Teledyne Geotech-Seismic Data Laboratory Report No. 264, Contract Number ARPA-AFTAC VELA T/2706, F33657-72-C-0009, Alexandria, Virginia.

Papoulis, Athanasios (1962) The Fourier Integral and its Applications, McGraw-Hill, New York.

Turin, George L. (1960) An Introduction to Matched Filters, I.R.E. Trans., IT-6, 311-329.